Mapping the Invasive Species Chinese Tallow

Elijah Ramsey III, Gene Nelson, Amina Rangoonwala, and Robert Ehrlich

Research into the use of Hyperion hyperspectral sensor data following the launch of EO-1 in November 2000, has made it possible to develop remote sensing tools to map localized occurrences and regional distribution of the widespread invasive species; Chinese tallow (*Sapium sebiferum)*. It is expected that these tools and accompanying methodologies will provide a template for mapping and monitoring a variety of invasive species in different geographic areas.

Since its introduction into the United States in the late 1700s, Chinese tallow (Figure 1) has spread from South Carolina to Florida and from Texas to Arizona and Southern California. It is continuing its rapid advance, and once it gains a foothold, removal is extraordinarily difficult. The best defense is an aggressive offense: detect early and eradicate. Its spread is creating extensive and irrevocable damage to native communities. The actual distribution of this menace has yet to be mapped even though such mapping is critical to the survival of many native habitats and wildlife. The ability to map its location would be critical both to documenting its spread and to eradication efforts and also to assessing the success of various controls. On a larger scale, identification by regional mapping and a method of regular monitoring are keys to addressing the infestation of all non-native plants within the United States.

Figure 1. Chinese tallow. Tree size varies, depending on age and site. It quickly can reach 10 to 14 meters tall. It is deciduous with extremely hardy and poisonous tissue. Plant is nonnative to the United States. Leaves are light to medium green, and fall leaves are yellow to rich red. Flowers are small, stalked, and white. Fruit is a seed with a durable woody three-lobed husk.

By all accounts, Chinese tallow is usually hard to detect. It mixes spectrally and structurally into the matrix of native plants. Further, pure stands of tallow trees are rare and where they do occur, the stands are rarely larger than 5 meters. In most instances, tallow trees are mixed intricately and at a low density among similar coastal and adjacent upland native vegetation.

The first attempt to map Chinese tallow with remote sensing data used airborne color-infrared (CIR) photography to simulate low spectral but high spatial resolution satellite and airborne image and digital video data (Ramsey III, E., G. Nelson, S. Sapkota, E. Seeger, and K. Martella, 2002. Mapping Chinese tallow with color-infrared photography. *Photogrammetric Engineering & Remote Sensing*, 68, 251-255). Mapping occurred when senescing Chinese tallow with its bright red leaves presented stood out in a high spectral contrast to its surrounding landscapes (Figure 2). To simulate low spectral but high spatial resolution satellite and airborne image and digital video data, CIR photography was scanned at a 1.0 m spatial resolution or less and classified for the occurrence of bright red leaves associated with senescing Chinese tallow. Classification accuracies greater than 95% confirmed that high spatial

resolution data could be used to monitor Chinese tallow infestations (Table 1), but the mapping was labor-intensive and spatial coverage was severely limited.

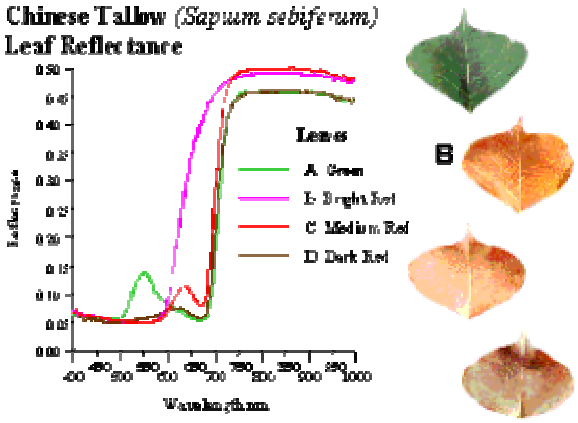

Figure 2. Examples of the various Chinese tallow leaf colors and associated reflectances

Table 1. Accuracy assessment of classified 0.5 and 1.0 m CIR photography

Commission Error: 50 randomly selected tallow trees from classified imagery compared to CIR photography

				CIR Photography			
			Resolution (m)	Tallow	Non-Tallow	Correct %	Commission %
Classified Imagery	Landcover Type	Bottom and Hardwood Forest	1.0-m	50	0	100	0
			0.5	49	1	98	2
		Upland Forest	1.0	46	4	92	8
			0.5	48	2	96	4
		Marsh	1.0	47	3	94	6
			0.5	50	0	100	0

Omission Error: 50 randomly selected tallow trees from CIR photography compared to classified imagery

				Classified Imagery			
			Resolution (m)	Tallow	Non-Tallow	Correct %	Omission %
Classified Imagery	Landcover Type	Bottom and Hardwood Forest	1.0-m	47	3	94	6
			0.5	49	1	98	2
		Upland Forest	1.0	47	3	94	6
			0.5	48	2	96	4
		Marsh	1.0	50	0	100	0
			0.5	45	5	90	10

To overcome this challenge, high spectral resolution data that offered subtle spectral discrimination was used to compensate for the use of moderate spatial resolution data that offered regional coverage. The Hyperion sensor provided the necessary high spectral resolution data at a reasonable cost, and a spectral unmixing tool provided the necessary subpixel Chinese tallow detection. Even with the appropriate hyperspectral data and spectral mapping tool, detecting the normally low percent occurrence of Chinese tallow within the matrix of native plants required identifying subtle spectral differences within the remote sensing image data. Atmospheric spectral leveling diminished the ability to determine subtle spectral differences, and therefore, to determine changes in canopy composition, in this case, tallow percent occurrence. Atmospheric removal allows extraction of the canopy reflectance from the sensor signal, maximizing the potential spectral distinctiveness (information, tallow percent occurrence) of each reflectance spectra.

To obtain the necessary subtle detection accuracy while maintaining spatially extensive coverage, a model strategy was generated and implemented that transformed Hyperion image data into accurate renditions of the canopy reflectance (Ramsey III, E., and G. Nelson, in review, A whole image approach for transforming EO-1 Hyperion hyperspectral data into accurate reflectance data with site-specific measurements). The model strategy accounted for atmospheric influences, the view and sun geometries, and illumination of the target and used a whole-image approach coupled with site-specific canopy reflected radiance measurements to transform the Hyperion apparent reflectance image data into highly accurate reflectance data (Figure 3).

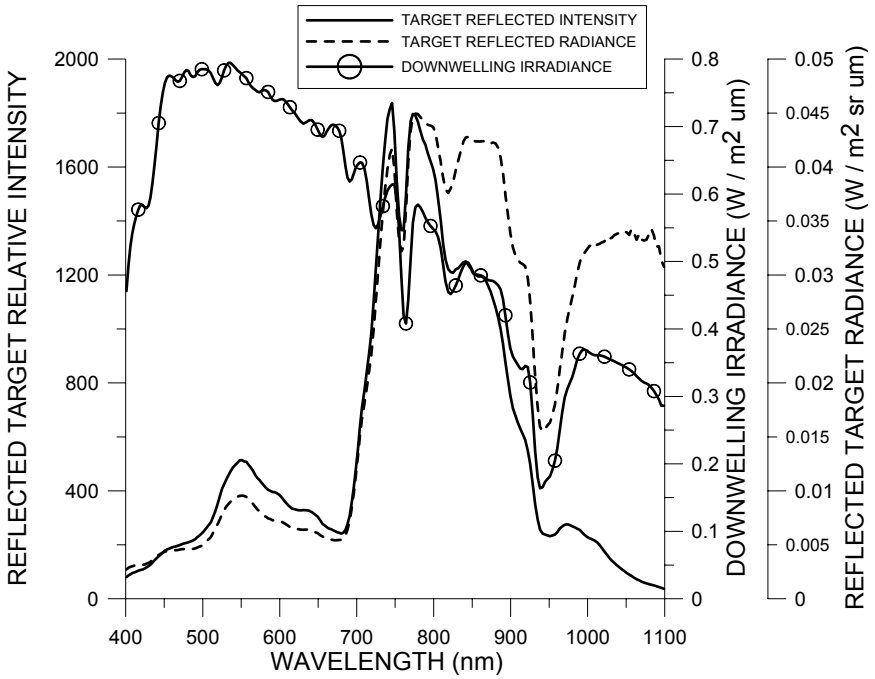

Figure 3. Measured downwelling irradiance at the time of the Hyperion image data collection. Measured upwelling intensity before and after calibration to radiance. Absorption features associated with water (about 930 nm to 960 nm) and oxygen (around 690 nm and 760 m) are shown in the recorded spectra.

Overall, hyperspectral reflectance spectra generated with the atmospheric correction and normalization model strategy followed expected spectral trends and contained expected prominent features. Differences in the observed and modeled canopy reflectance spectra were usually low or nearly non-

existent. Where relatively higher differences existed, these were most likely associated with problems in the comparison, not in the model generation. Typical differences between the observed (site-specific) and modeled (Hyperion) reflectances would be expected to range from ±1.0% to ±1.6% in the visible and ±5% in the near infrared wavelengths in 95% of the model simulations. These comparisons verified that this strategy successfully produced highly accurate and detailed renditions of canopy reflectances when Hyperion data was collected. The high accuracy supplied the highest spectral detail possible necessary for the subtle spectral discrimination and detection of the red Chinese tallow leaves in the matrix of native vegetation.

Once accurate spectral detail was obtained, an algorithm operating on the Hyperion corrected and normalized canopy reflectance data was used to provide realistic and predictive characteristic spectra that represented the percent occurrence of pertinent land cover spectral characteristics occurring during Hyperion image collection (Ramsey III, E., G. Nelson, R. Ehrlich, A. Rangoonwala and K. Martella, in review, Generation and validation of characteristic spectra from EO1 Hyperion image data for detecting the percent occurrence of invasive species, specifically Chinese Tallow). Collected leaf spectra provided evidence for the expected forms of canopy reflectance spectra that characterized the pertinent land covers. Site-specific canopy reflectance spectra also directly linked the site composition variance directly influencing the canopy reflectance and the canopy reflected radiance measured at the sensor. Simultaneous collection and subsequent classification of 35-mm slides provided dominant site-specific compositions at the time of the Hyperion image data collection. Mixing proportions associating the modeled characteristic spectra with the site compositions were compared with compositions generated from the slide classifications. This final comparison ensured that the modeled characteristic spectra adequately portrayed the dominant canopy reflectance variance existent during image collection.

Using the input site-specific reflectance spectra sets, the sub pixel extraction model found five characteristic spectra that adequately represented the site-specific and also the corresponding Hyperion imaged canopy reflectance spectra data sets. The sets of spectra were similar (Figures 4 and 5). One characteristic spectrum represented the percent occurrence of senescing cypress-tupelo and leaf-off and brown foliage. Two others represented the percent of shadows and green vegetation occurrences. The shadow and green vegetation variances were correlated. The fourth characteristic spectrum was somewhat related to the percent of yellow tallow and yellowing foliage.

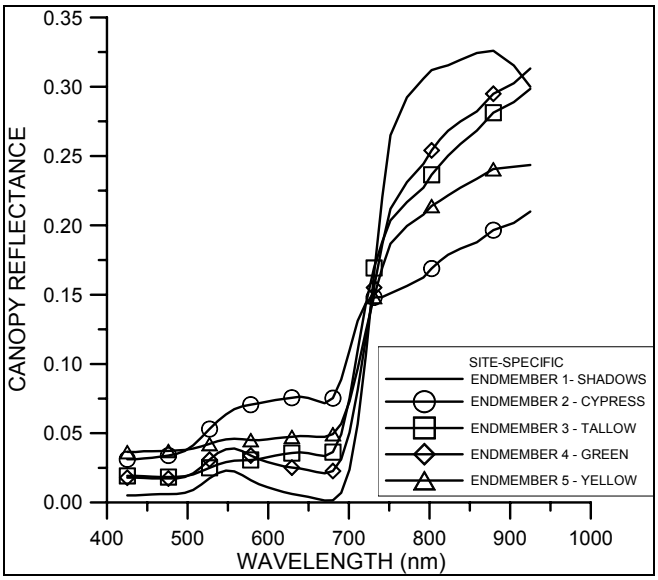

Figure 4. Site-specific characteristic spectra extracted from site-specific canopy rerflectance spectra. (Legend: line: canopy shadows, circle: senescing foliage and senescing Cypress, square: red Chinese tallow, diamond: green vegetation, and triangle: yellow Chinese tallow but mostly noise.)

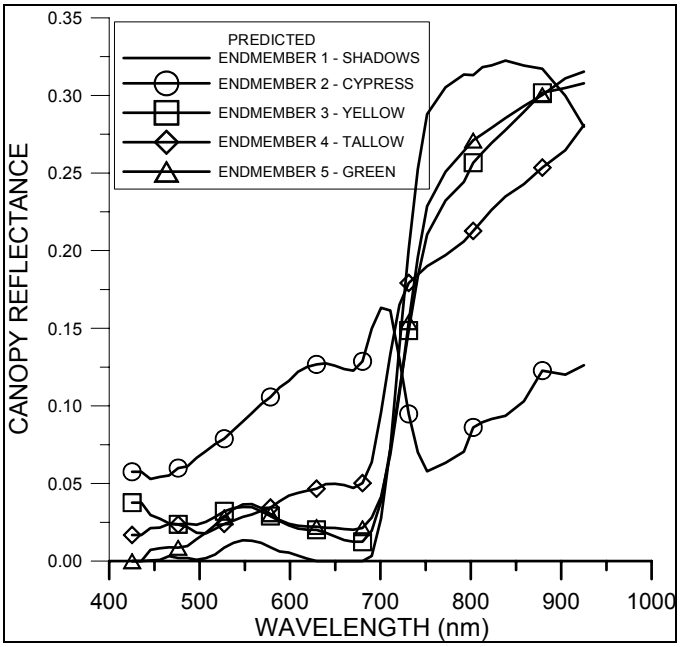

Figure 5. Image characteristic spectra extracted from Hyperion image canopy reflectance spectra (corrected for atmospheric influences). Line: canopy shadows, circle: senescing foliage and senescing Cypress, square: red Chinese tallow, diamond: green vegetation, and triangle: yellow Chinese tallow but mostly noise.

The final characteristic spectrum was visually and statistically associated with the percent of red Chinese tallow. About 81% and 78% of the composition variances associated with the red tallow site-specific and imaged characteristic spectra, respectively, were explained by the site-specific compositions generated in the site-specific slide classification (Figures 6 and 7). The implemented methodology, including validation and verification, ensured the modeled characteristic spectra were both physically realistic and predictive, and thereby these spectra could more likely be spatially and temporally extended and used with other sources of hyperspectral sensor image data.

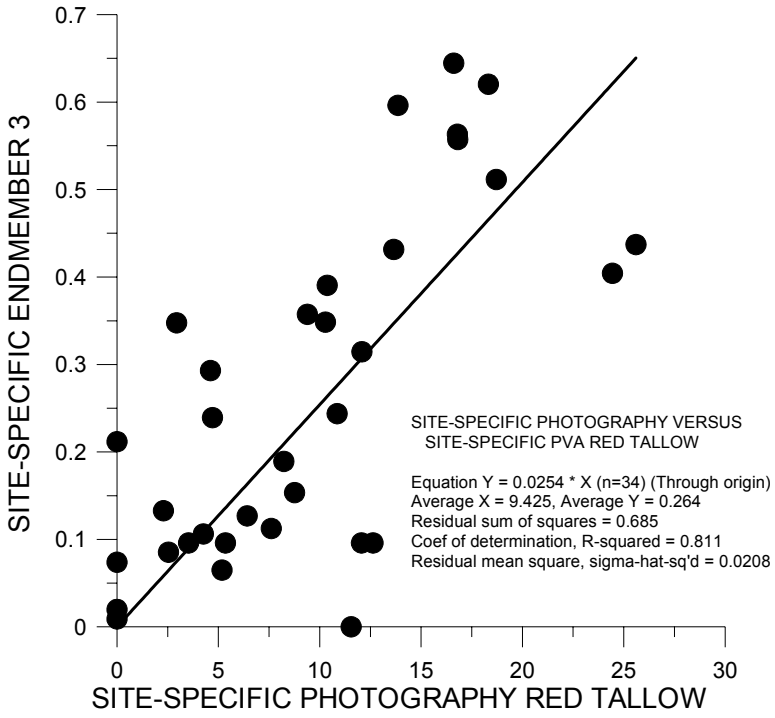

Figure 6. Site-specific percent compositions generated from classification of 35-mm slides taken from a helicopter near the time of Hyperion image collection plotted vs. the compositions extracted from site-specific reflectance spectra with the generated red tallow site-specific characteristic spectra (Figure 4).

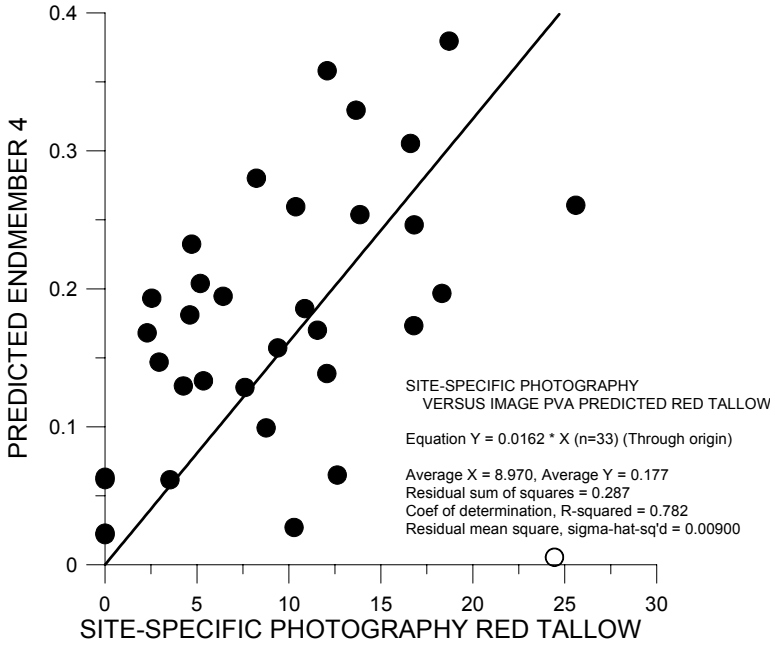

Figure 7. Site-specific percent compositions generated from classification of 35-mm slides taken from a helicopter near the time of Hyperion image collection plotted vs. compositions extracted from Hyperion image reflectance spectra with generated red tallow image based characteristic spectra (Figure 5).

The final objective was to implement methods designed and tested in the previous studies and provide a realistic and accurate representation of the spatial distribution of the percent of Chinese tallow within the Hyperion coverage. Using results generated in the previous studies, corrected and normalized Hyperion reflectance image data were transformed into composition images with a subpixel extraction model (Ramsey III, E. A. Rangoonwala, G. Nelson, and R. Ehrlich, in review, Mapping the invasive species, Chinese Tallow with EO1 satellite Hyperion hyperspectral image data and relating tallow

percent occurrences to a classified Landsat Enhanced Thematic Mapper Plus landcover map). Composition images were related to green vegetation (combining the green and shadow characteristic spectra), senescent foliage and senescing cypress-tupelo forest, red Chinese tallow, and a final composition image that was slightly related to yellow tallow but mostly did not correspond to any observed land cover feature. Statistical and visual comparisons confirmed successful portrayal of these landscape features at the time of Hyperion image collection (Figure 8).

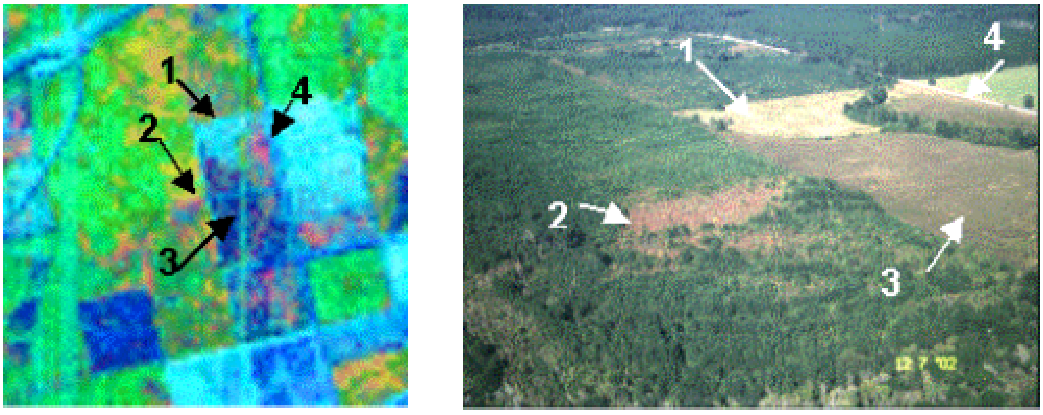

Figure 8. Slide and color composite of image related to the percent of green vegetation, senescent foliage, and senescing cypress-tupelo forest (blue), and red Chinese tallow (red). This image shows a pine seedling nursery surrounded by cultivated and fallow fields and mature pine forests.

In a final analysis, the percent occurrence of red tallow as a surrogate for Chinese tallow was linked to land covers generated with Landsat Enhanced Thematic Mapper Plus (ETM+) image data as a first step to establish the sensitive and susceptible of various ecosystems to risk of invasive establishment (Figure 9). Results suggested that the highest percent and widest distribution of tallows were located (1) on the numerous and ubiquitous topographic highs and levies within and lining the coastal canals, (2) scattered throughout fallow fields or along fence rows separating active and non active fields, and (3) in disturbed or more open canopy woody wetland deciduous forests (including cypress-tupelo forests), upland woody land evergreen forests (dominantly pines), and upland deciduous and mixed forests. Additionally, pine and in one case cypress plantations were often highly contaminated by tallow trees. In all, narrow linear features (levies, fencelines, cheniers) and scattered trees and small isolated stands were mixed with the native vegetation in the ETM+ pixel and amalgamated within the land cover classification. Newly created remote sensing techniques relying on Hyperion hyperspectral image data and a specialized subpixels extraction model provided identification of subtle spectral anomalies caused by the occurrence of red tallow that was not possible with the coarser spectral resolution Landsat ETM+ image data. Linkage of these occurrences with the ETM+ land cover map dramatized those ecosystems containing the highest levels of tallow and those activities that enhanced tallow establishment.

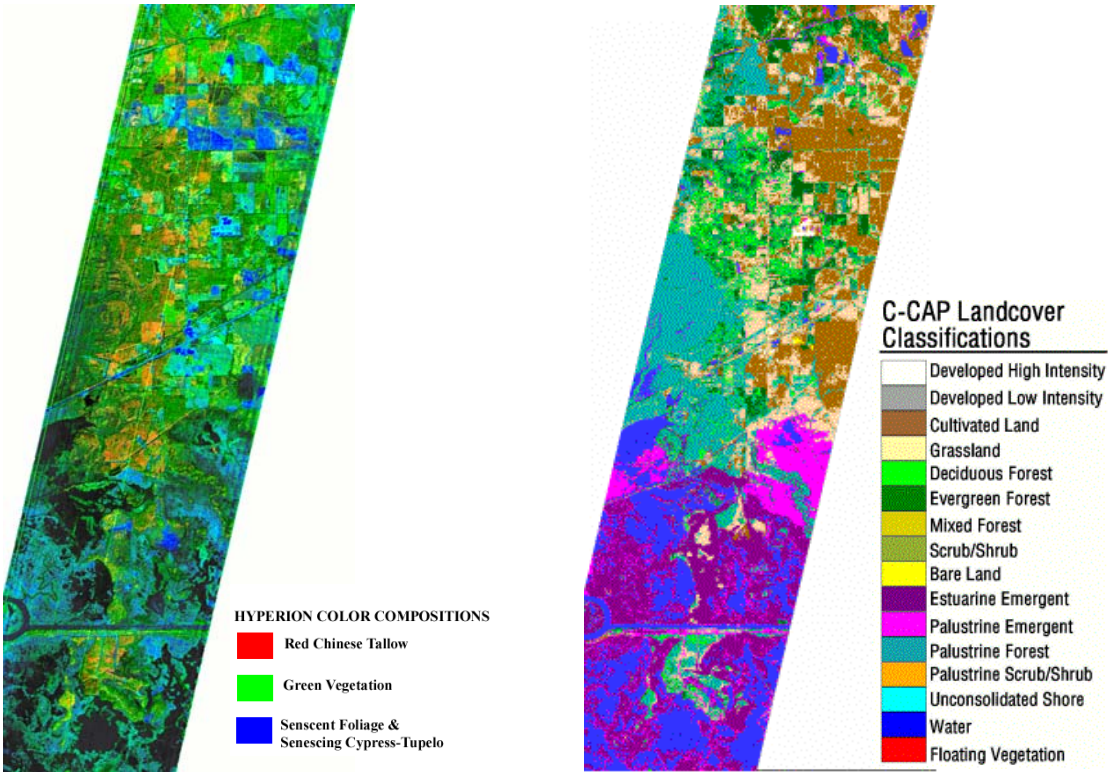

Figure 9. (Left) Hyperion composition images related to the percent occurrence of green vegetation (green color), senescent foliage, and senescing cypress-tupelo forest (blue color), and red Chinese tallow (red color). (Right) The same area classified following C-CAP protocols and by using Landsat ETM+ image data. (Ramsey et al. 2001, Ramsey and Nelson in review).

Conclusion:

Use of Hyperion sensor data enabled the occurrence of senescing (red) Chinese tallow to be estimated and mapped in the study area.